Blind Modulation Classification for Asynchronous OFDM Systems Over Unknown Signal Parameters and Channel Statistics

Rahul Gupta, Sushant Kumar, and Sudhan Majhi, *Senior Member, IEEE*

***Abstract*—Blind modulation classification (MC) is an integral part of designing an adaptive or intelligent transceiver for future wireless communications. However, till date, only a few works have been reported in the literature for blind MC of orthogonal frequency division multiplexing (OFDM) system over frequency-selective fading environment. In this paper, a blind MC algorithm has been proposed and implemented over National Instruments (NI) testbed setup for linearly modulated signals of OFDM system by using discrete Fourier transform (DFT) and normalized fourth-order cumulant. The proposed MC algorithm works in the presence of synchronization errors, i.e., frequency, timing, and phase offsets and without the prior information about the signal parameters and channel statistics. To nullify the effect of timing offset in the feature extraction process, a statistical average has been taken over OFDM symbols after introducing uniformly distributed random timing offsets in each of the OFDM symbols. In this work, we have classified a more extensive pool of modulation formats for OFDM signal, i.e., binary phase-shift keying (BPSK), quadrature PSK (QPSK), offset QPSK (OQPSK), minimum shift keying (MSK), and 16 quadrature amplitude modulation (16-QAM). Classification is performed in two stages. At the first stage, a normalized fourth-order cumulant is used on the DFT of the received OFDM signal to classify OQPSK, MSK, and 16-QAM modulation formats. At the second stage, first we compute the DFT of the square of the received OFDM signal and then a normalized fourth-order cumulant is used to classify BPSK and QPSK modulation formats. The success rate of the proposed MC algorithm is evaluated through analytical and Monte Carlo simulations and compared with existing methods. Finally, the work is validated by providing an experimental setup on NI hardware over an indoor propagation environment.**

***Index Terms*—Blind modulation classification, discrete Fourier transform, fourth-order cumulant, orthogonal frequency division multiplexing, testbed implementation.**

I. Introduction

BLIND modulation classification (MC) identifies the modulation format of the received signal and ensures correct demodulation to retrieve the transmitted data [1]. It plays an essential role in numerous military and civilian applications such as signal intelligence, signal monitoring, cognitive radio, and software-defined radio [2]–[4]. Blind parameter estimation and classification algorithms can be used with an intelligent receiver, resulting in a significant improvement in the spectral efficiency, as no predefined training or pilot sequence is required [5], [6]. Orthogonal frequency division multiplexing (OFDM) is a well-known multicarrier modulation technology for future wireless communication systems. The key advantage of OFDM is the ability to cope with severe channel conditions. Hence, the OFDM technique has been used as the main transmission scheme over frequency-selective fading channels [7]. Classification of modulation formats for OFDM signal is an important research problem for the fifth generation (5G) and beyond wireless communication, where artificial intelligence will be an integral part of physical layer communication [8]–[11].

In the past decades, various MC algorithms have been developed for single-carrier systems that can be categorized into likelihood-based (LB) and feature-based (FB) methods [1]. The MC for single-carrier systems has been widely investigated in [1]–[3], [12]–[18]. The LB algorithms are optimal in the Bayesian sense, but they suffer from high computational complexity [12]. They also require prior knowledge of the signal parameters for the identification of modulation formats, which is usually not desirable for an intelligent or adaptive transceiver. On the other hand, FB algorithms usually yield a sub-optimal solution. They are generally easier to implement and have lower computational complexity and also do not require prior knowledge of the signal parameters and channel statistics. The FB algorithms, such as cumulants [13], [14], cyclic statistics [2], [3], [15]–[17] and wavelet transforms [18] extract unique features to recognize the modulation formats. The MC algorithms based on cumulants and moments are used to classify M-ary phase-shift keying (M-PSK) and M-ary quadrature amplitude modulation (M-QAM) modulation formats. It employs threshold values to differentiate the features. Hence, it is easier to implement and works well in the presence of additive white Gaussian noise (AWGN) and fading channels [13], [14]. The higher-order cyclic statistics-based algorithms [2], [3], [15]–[17] are robust and perform well even in flat and frequency-selective fading channels. They use non-zero cycle frequencies of the received signals to recognize M-PSK/M-QAM modulation formats. The MC algorithm for multiple-antenna systems is studied in [2]

Manuscript received July 12, 2019; revised December 14, 2019; accepted March 1, 2020. Date of publication March 19, 2020; date of current version May 14, 2020. This work was supported in part by the Visvesvaraya Young Faculty Research Fellowship, Ministry of Electronics and Information Technology, Government of India, being implemented in part by the Digital India Corporation, in part by Early Career Young Scientists and the Empowerment and Equity Opportunities for Excellence in Science schemes and in part by the Science and Engineering Research Board under the Department of Science and Technology, Government of India. The review of this article was coordinated by Prof. H. H. Nguyen. *(Corresponding author: Sudhan Majhi.)*

The authors are with the Department of Electrical Engineering, Indian Institute of Technology Patna, Bihar 801103, India (e-mail: rahul.pee15@iitp.ac.in; sushant.pee15@iitp.ac.in; smajhi@iitp.ac.in).

Digital Object Identifier 10.1109/TVT.2020.2981935

0018-9545 © 2020 IEEE. Personal use is permitted, but republication/redistribution requires IEEE permission.
See https://www.ieee.org/publications/rights/index.html for more information.

Authorized licensed use limited to: Indian Institute of Technology Patna. Downloaded on January 16,2024 at 05:46:31 UTC from IEEE Xplore. Restrictions apply.

based on the combination of higher-order correlation, cyclic cumulant, and cumulant. The algorithm discussed in [3] is for single antenna and single-carrier systems. It employs the combined properties of cumulant and cyclic cumulants and works well over flat fading channels. In addition, [2] and [3] can also able to classify different variants of quadrature PSK (QPSK), i.e., offset QPSK (OQPSK), minimum shift keying (MSK), and $\pi/4$-QPSK modulation formats.

Over the last few years, MC algorithms based on machine learning and deep learning (DL) have also gained attention [19]–[25]. The MC algorithm based on genetic programming (GP) and K-nearest neighbor is studied in [19]. Cumulants are used as input features for GP to classify modulation formats. The extreme learning machine and higher-order statistical based MC algorithm for multiple antenna systems is given in [20]. The DL-based method discussed in [21], [22] is combined with two convolutional neural networks (CNNs) that have the ability to classify modulation formats even in scenarios with a low signal-to-noise ratio (SNR). Besides, CNN-based MC algorithms have the certain robustness to estimation error on carrier phase offset and SNR. The method discussed in [23] extract distinct features using higher-order cumulants, and then the deep neural network (DNN) model was designed to classify modulation formats based on these features. Nevertheless, the methods discussed above [1]–[3], [12]–[23] are limited to single-carrier systems only. Moreover, the algorithms for OFDM and multiple-input multiple-output OFDM systems based on DNN and Gibbs sampling are explored in [24]–[26]. Furthermore, these algorithms are limited to known channel and/or perfect synchronization conditions.

In the literature, there are a very few MC algorithms exist for the OFDM systems [27]–[31]. The likelihood and maximum a-posteriori [27] based MC algorithm works with known channel state information (CSI). The likelihood-based index modulation studied in [28] works for both known and unknown CSI. However, both algorithms consider the OFDM system to be perfectly synchronized to classify M-PSK / M-QAM modulation formats. The Kolmogorov-Smirnov (KS) based method discussed in [29] is a non-parametric approach to classify M-PSK/M-QAM modulation formats. It works in the presence of known timing offset and unknown frequency and phase offsets, as well as for the non-Gaussian noise channel. The MC algorithm based on the statistical properties of the received OFDM signal is discussed in [30]. This algorithm discriminates the features of QPSK, 16-QAM, and 64-QAM modulation formats by employing mean, skewness, and kurtosis. However, this algorithm does not work well in the presence of timing and frequency synchronization errors. The MC algorithm using amplitude moments is studied in [31]. This method uses the correlation between any two subcarriers to classify 16-QAM and 64-QAM modulation formats. The MC algorithms for the OFDM signal discussed in [24], [27]–[31] are limited to known channel and/or perfect synchronization conditions. To the best of the author's knowledge, there is no blind MC algorithm for OFDM systems that has been proposed and implemented over realistic scenarios and in the presence of synchronization errors, i.e., timing, frequency, and phase offsets with unknown signal parameters and channel statistics. Moreover, classifying QPSK, OQPSK, and MSK together for OFDM system is another major problem.

In this work, we propose a blind MC algorithm for linearly modulated signals of the OFDM systems. The proposed modulation classifier has important features, discussed as

- In the proposed MC algorithm, unique features are acquired to classify a more extensive pool of modulation formats, i.e., binary PSK (BPSK), QPSK, MSK, OQPSK, and 16-QAM.
- The features are extracted by using the combined properties of discrete Fourier transform (DFT) and the normalized fourth-order cumulant of the received OFDM signal.
- The proposed MC is applicable to OFDM systems in the presence of timing, frequency, and phase offsets. Since it does not require any prior knowledge of signal parameters and channel statistics, it is completely a blind process.
- The performance of the proposed modulation classifier is robust over flat and frequency-selective fading channel.
- The computational complexity and performance of the proposed MC algorithm have been compared with some existing MC methods.
- To authenticate the proposed MC algorithm, analytical, Monte Carlo simulations, and experiment is performed on the National Instruments (NI) testbed over an indoor propagation environment.

The rest of the paper is arranged as follows: The signal model of the received OFDM system is given in Section II. Then the proposed MC algorithm is presented in Section III using the combined properties of DFT and normalized fourth-order cumulant. It includes feature extraction, selection, and complexity analysis. The testbed implementation and measurement setup are provided in Section IV. Section V illustrates the simulation and measurement results. Finally, conclusions are drawn in Section VI.

II. OFDM Signal Model

In this section, we consider an OFDM system with N_0 subcarriers, the samples of an mth OFDM symbol are generated by using N-point inverse DFT (IDFT) and can be expressed as

$$s_m[k] = \sum_{n=0}^{N-1} S_m[n] e^{j2\pi nk/N}, \quad 0 \le k \le N-1, \tag{1}$$

where $N = \rho \times N_0$, ρ is the oversampling factor, $S_m[n]$ is the modulated data and can be written as

$$S_m[n] = \begin{cases} \bar{S}_m[n] & 0 \le n \le N_0/2 - 1 \\ \bar{X} & N_0/2 \le n \le N_0(\rho - 1/2) - 1 \\ \bar{S}_m[n] & N_0(\rho - 1/2) \le n \le N - 1, \end{cases} \tag{2}$$

where $\bar{S}_m[n]$ is the modulated information of mth OFDM symbol and $\bar{X}$ is the zeros padding vectors of length $N_0(\rho - 1)$. The cyclic prefix (CP) of length N_{cp} is added in front of $s_m[k]$ for mitigating the effect of intersymbol interference (ISI). The transmitted baseband signal can be obtained as

$$\bar{s}_m[k] = \begin{cases} s_m[k+N], & -N_{cp} \le k \le -1 \\ s_m[k], & 0 \le k \le N-1. \end{cases} \tag{3}$$

Authorized licensed use limited to: Indian Institute of Technology Patna. Downloaded on January 16,2024 at 05:46:31 UTC from IEEE Xplore. Restrictions apply.

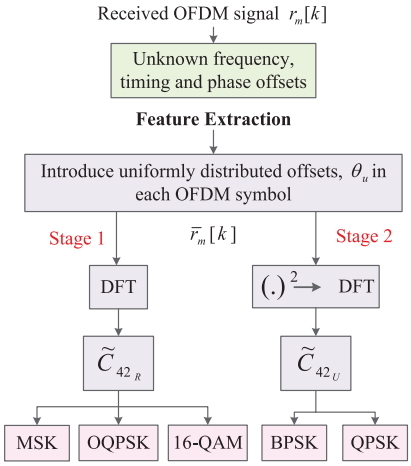

Fig. 1. Block diagram of the proposed blind modulation classification using DFT and the normalized fourth-order cumulant for OFDM system.

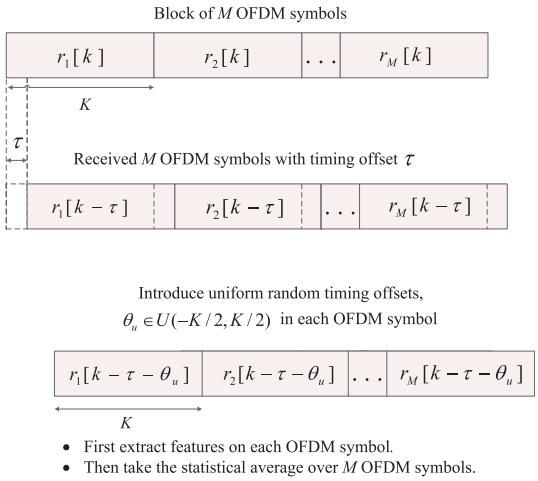

Fig. 2. OFDM transmission, reception, and timing offset compensation analysis in the proposed MC algorithm.

The received OFDM signal over a frequency-selective fading channel can be expressed as

$$r_m[k] = e^{j(2\pi f_o k/N+\phi)} \sum_{l=0}^{L-1} h[l]\, \bar{s}_m[k-l-\tau]_{\text{mod}K} + w[k], \quad 0 \le k \le K-1, \tag{4}$$

where f_o is the frequency offset normalized by the subcarrier spacing $1/T$ (T is an OFDM symbol interval), ϕ is the phase offset, τ is the timing offset due to the wireless channel, $w[k]$ is the AWGN with zero mean and variance σ_w^2, and K is the received signal length, $K = N + N_{cp}$. The channel impulse response (CIR) of the frequency-selective fading channel is denoted by $h[l]$, where $l = 0, 1, \ldots, L-1$ and L is the length of the CIR, providing $N_{cp} \ge L$.

III. Proposed Blind Modulation Classification

In this work, we propose a blind MC algorithm for linearly modulated signals of the OFDM system. The proposed blind MC algorithm is able to classify a more comprehensive pool of modulation formats, i.e., BPSK, QPSK, MSK, OQPSK, and 16-QAM, in the presence of timing, frequency, and phase offsets. It utilizes the combined properties of DFT and the normalized fourth-order cumulant of the received OFDM signal as shown in Fig. 1. The proposed algorithm uses fourth-order cumulant, however, it is totally different from our previous MC algorithms which work only for single carrier system [2], [3]. Hence, our previous MC algorithms are not applicable for OFDM system. Moreover, the MC in [2] and [3] uses cyclic cumulants to extract features, i.e., positions of non-zero cycle frequencies (symbol rate frequency or intermediate frequency) of the received signals. On the other hand, OFDM cannot employ cyclic cumulants to classify the modulation formats because of the concept of multiple subcarriers.

A. Feature Extraction

The modulated information $S_m[n]$ of the OFDM signal is in the frequency domain. Hence, the feature extraction process of the proposed MC algorithm also uses a frequency domain signal. Fig. 2 shows the OFDM transmission, reception, and timing offset compensation analysis in the proposed MC algorithm. The first topmost sub-figure shows a block of M OFDM symbols, where K is the sample length of each OFDM symbol. The second sub-figure shows the M received OFDM symbols with timing offset τ. The timing offset τ is fixed for an OFDM block and is therefore fixed for each OFDM symbol in a particular block. However, it may vary from block to block. Any feature that depends on τ will also vary from block to block, hence an appropriate threshold value cannot be specified. Thus to nullify the effect of timing offset in the feature extraction process, we introduce uniform random timing offsets $\theta_u \in \mathcal{U}(-K/2, K/2)$ in each OFDM symbol, as shown at the bottom of Fig. 2. Moreover, the frequency offset creates inter carrier interference within the OFDM sysmbol, hence the total power remains the same for the OFDM symbol unless frequency offset is very high. Therefore, the normalized fourth-order cumulant with two conjugations in the frequency domain cancels the phase and frequency offset effect. The overall OFDM sample length K can be easily estimated by using the cyclic correlation function in [32]. Now, we can write the modified expression for the mth OFDM symbol as

$$\bar{r}_m[k] = r_m\left[k-\tau-\theta_u\right], \quad 0 \le k \le K-1.$$

1) First Stage Classification: At the first stage, the normalized fourth-order cumulant is used on the DFT of the received OFDM signal to classify OQPSK, MSK, and 16-QAM modulation formats. The DFT of the mth OFDM symbol, $\bar{r}_m[k]$, is obtained as

$$\begin{aligned} \bar{R}_m[v] &= \sum_{k=0}^{K-1} \bar{r}_m[k] e^{-j2\pi kv/K}, \quad 0 \le v \le K-1, \\ &= \sum_{k=0}^{K-1} r_m\left[k-\tau-\theta_u\right] e^{-j2\pi kv/K}, \\ &= e^{-j2\pi v/K(\tau+\theta_u)} R_m[v], \end{aligned} \tag{5}$$

Authorized licensed use limited to: Indian Institute of Technology Patna. Downloaded on January 16,2024 at 05:46:31 UTC from IEEE Xplore. Restrictions apply.

where $R_m[v]$ is the DFT of the received OFDM signal $r_m[k]$. For random processes $\bar{R}_{m_1}[v], \ldots, \bar{R}_{m_x}[v]$, the xth-order joint moment and cumulant are defined as [33]

$$M_{x_{\bar{R}_{m_1}[v],\ldots,\bar{R}_{m_x}[v]}} = E\left[\prod_{a=1}^{x} \bar{R}_{m_a}[v]\right], \tag{6}$$

$$C_{x_{\bar{R}_{m_1}[v],\ldots,\bar{R}_{m_x}[v]}} = \sum (-1)^{p-1}(p-1)!\, E\left[\prod_{a\in\varrho_1} \bar{R}_{m_a}[v]\right] \times \ldots E\left[\prod_{a\in\varrho_p} \bar{R}_{m_a}[v]\right], \tag{7}$$

where the summation extends over all partitions $(\varrho_1, \ldots, \varrho_p)$, $p = 1, \ldots, x$, of $(1, \ldots, x)$. When $\bar{R}_{m_a} = \bar{R}_m$, $a = 1, \ldots, x$, this gives the xth-order moment as $M_{x_{\bar{R}_m}} = E[\bar{R}_m[v]^x]$. For complex-valued random processes, mixed moments are defined according to the conjugation placements. The mixed moment of order x with y conjugations for $\bar{R}_m[v]$ is defined as

$$M_{xy_{\bar{R}_m}} = E\left[\bar{R}_m[v]^{x-y}\, \bar{R}_m^*[v]^y\right]. \tag{8}$$

The xth-order cumulants and mixed cumulants with y conjugations can be defined accordingly as in (7). Throughout the paper, the cumulants of most interest are fourth-order. The sample average of the fourth-order cumulant of (5) with two conjugations is obtained as

$$\begin{aligned}\hat{C}_{42_{\bar{R}_m}} &= \frac{1}{K}\sum_{v=0}^{K-1}\left|e^{-j2\pi v/K(\tau+\theta_u)} R_m[v]\right|^4 \\ &\quad - \left|\frac{1}{K}\sum_{v=0}^{K-1} e^{-j4\pi v/K(\tau+\theta_u)} R_m^2[v]\right|^2 \\ &\quad - 2\left(\frac{1}{K}\sum_{v=0}^{K-1}\left|e^{-j2\pi v/K(\tau+\theta_u)} R_m[v]\right|^2\right)^2, \\ &= \vec{C}_{42_{R_m}} - \left|\frac{1}{K}\sum_{v=0}^{K-1} e^{-j4\pi v/K(\tau+\theta_u)} R_m^2[v]\right|^2, \end{aligned} \tag{9}$$

where $\vec{C}_{42_{R_m}} = \frac{1}{K}\sum_{v=0}^{K-1}|R_m[v]|^4 - 2(\frac{1}{K}\sum_{v=0}^{K-1}|R_m[v]|^2)^2$. It is noted that the above cumulant has the form of the sum of signal and noise. In practice, we estimate the normalized fourth-order cumulant by

$$\tilde{C}_{42_{\bar{R}_m}} = \frac{\vec{C}_{42_{R_m}} - \left|\frac{1}{K}\sum_{v=0}^{K-1} e^{-j4\pi v/K(\tau+\theta_u)} R_m^2[v]\right|^2}{\frac{1}{K}\sum_{v=0}^{K-1}|R_m[v]|^2 - C_{21,W}}, \tag{10}$$

where $C_{21,W} = \sigma_W^2$ is an estimated variance of AWGN. In the testbed implementation, we estimate $C_{21,W}$ from a receiver system noise floor through a calibration process. Now we take the average of all cumulant values, i.e., equal to the total number of OFDM symbols M, given as

$$\tilde{C}_{42_R} = \frac{1}{M}\sum_{m=1}^{M} \frac{\vec{C}_{42_{R_m}} - \left|\frac{1}{K}\sum_{v=0}^{K-1} e^{-j4\pi v/K(\tau+\theta_u)} R_m^2[v]\right|^2}{\frac{1}{K}\sum_{v=0}^{K-1}|R_m[v]|^2 - C_{21,W}}. \tag{11}$$

The above equation (11), gives distinct values for OQPSK, MSK, and 16-QAM. Hence, modulation formats OQPSK, MSK, and 16-QAM can be classified by defining appropriate threshold values, discussed in Section III-B. However, the above average normalized fourth-order cumulant gives the same value for BPSK and QPSK modulation formats.

2) Second Stage Classification: To classify BPSK and QPSK modulation formats, we use the DFT of the square of the received OFDM signal and then apply the normalized fourth-order cumulant. The DFT of the square of the OFDM symbol, $\bar{r}_m^2[k]$, can be expressed as

$$\begin{aligned}\bar{U}_m[v] &= \sum_{k=0}^{K-1} r_m^2[k-\tau-\theta_u]\, e^{-j2\pi kv/K}, \\ &= e^{-j2\pi v/K(\tau+\theta_u)} U_m[v], \end{aligned} \tag{12}$$

where $U_m[v] = R_m[v] \circledast R_m[v]$, $\circledast$ is the linear convolution operation. Similar to (9), we find the sampled estimates of the fourth-order cumulant with two-conjugations of $\bar{U}_m[v]$ as

$$\hat{C}_{42_{U_m}} = \vec{C}_{42_{U_m}} - \left|\frac{1}{K}\sum_{v=0}^{K-1} e^{-j4\pi v/K(\tau+\theta_u)} U_m^2[v]\right|^2, \tag{13}$$

where $\vec{C}_{42_{U_m}} = \frac{1}{K}\sum_{v=0}^{K-1}|U_m[v]|^4 - 2(\frac{1}{K}\sum_{v=0}^{K-1}|U_m[v]|^2)^2$.

Now, the normalized fourth-order cumulant is obtained as

$$\tilde{C}_{42_{U_m}} = \frac{\vec{C}_{42_{U_m}} - \left|\frac{1}{K}\sum_{v=0}^{K-1} e^{-j4\pi v/K(\tau+\theta_u)} U_m^2[v]\right|^2}{\frac{1}{K}\sum_{v=0}^{K-1}|U_m[v]|^2 - C_{21,W}}, \tag{14}$$

Similarly, we take the average of M cumulant values as

$$\tilde{C}_{42_U} = \frac{1}{M}\sum_{m=1}^{M} \frac{\vec{C}_{42_{U_m}} - \left|\frac{1}{K}\sum_{v=0}^{K-1} e^{-j4\pi v/K(\tau+\theta_u)} U_m^2[v]\right|^2}{\frac{1}{K}\sum_{v=0}^{K-1}|U_m[v]|^2 - C_{21,W}}. \tag{15}$$

The above equation (15), gives distinct values for BPSK and QPSK modulation formats, hence, these can easily be classified by using a proper threshold value, discussed in Section III-B.

B. Feature Selection

In this section, features are discriminated based on the threshold values obtained by using the normalized fourth-order cumulant for the different modulation formats. Now to develop thresholds for the different modulation schemes, we need to derive expressions for the mean and variance of the sample estimates of the normalized fourth-order cumulant. For the ease of representation, we can write the generalized fourth-order cumulant of $\{\tilde{C}_{42_{\bar{R}_m}}$ or $\tilde{C}_{42_{\bar{U}_m}}\}$ as $\tilde{C}_{42}$ and moment of $\{M_{42_{\bar{R}_m}}$ or $M_{42_{\bar{U}_m}}\}$ as M_{42} and same for second-order statistics. The general expressions for mean, variance, and co-variance of the sample estimates of the second and fourth-order cumulant expressions

Authorized licensed use limited to: Indian Institute of Technology Patna. Downloaded on January 16,2024 at 05:46:31 UTC from IEEE Xplore. Restrictions apply.

obtained in (16)–(22); and are provided in the Appendix A. By using Taylor series approximation, the second-order estimator of the mean value of the generalized fourth-order cumulants, $\tilde{C}_{42}$, is expressed as [34]

$$E\left[\tilde{C}_{42}\right] = E\left[\frac{\hat{C}_{42}}{\tilde{C}_{21}^2}\right] = \frac{E\left[\hat{C}_{42}\right]}{E\left[\tilde{C}_{21}^2\right]}\left[1 - \frac{Cov\left[\hat{C}_{42}, \tilde{C}_{21}^2\right]}{E\left[\hat{C}_{42}\right] E\left[\tilde{C}_{21}^2\right]} + \frac{Var\left[\tilde{C}_{21}^2\right]}{E\left[\tilde{C}_{21}^2\right]^2}\right]. \quad (16)$$

The asymptotic mean value of the generalized fourth-order cumulant, $\hat{C}_{42}$, is given as (A.5)

$$E\left[\hat{C}_{42}\right] = M_{42}\frac{K-3}{K} - \left(|M_{20}|^2 + 2M_{21}^2\right)\frac{K-1}{K}. \quad (17)$$

Now, the asymptotic mean value of the generalized second-order cumulant, $\tilde{C}_{21}$, is obtained as (A.6)

$$E\left[\tilde{C}_{21}^2\right] = \frac{1}{K}\left[M_{42} + (K-1)M_{21}^2\right] + \sigma_W^4 - 2\sigma_W^2 M_{21}. \quad (18)$$

Similarly, the derivation of co-variance and variance are also provided in the Appendix A and the final expressions for the second and fourth-order cumulant are expressed as (A.16), (A.17)

$$Var\left[\tilde{C}_{21}^2\right] \approx \left(M_{21} - \sigma_W^2\right)^2 \frac{M_{42} - M_{21}^2}{K}. \quad (19)$$

$$Cov\left[\hat{C}_{42}, \tilde{C}_{21}^2\right] \approx \frac{2M_{63}M_{21}}{K} - \frac{10M_{42}M_{21}^2}{K} + \frac{8M_{21}^4}{K} - \sigma_W^2\left(\frac{2M_{63}}{K} + \frac{10M_{42}M_{21}}{K} - \frac{8M_{21}^3}{K}\right). \quad (20)$$

Substituting the values obtained from (17)–(19) into (16), we calculated the final expression of the mean of the estimated normalized cumulant $\tilde{C}_{42}$. Again, by using the Taylor series approximation, the general expression of the first-order estimator of the variance of the normalized fourth-order cumulant, $\tilde{C}_{42}$ is obtained as [34]

$$Var\left[\tilde{C}_{42}\right] = Var\left[\frac{\hat{C}_{42}}{\tilde{C}_{21}^2}\right] = \frac{E\left[\hat{C}_{42}\right]^2}{E\left[\tilde{C}_{21}^2\right]^2}\left[\frac{Var\left[\hat{C}_{42}\right]}{E\left[\hat{C}_{42}\right]^2} - 2\frac{Cov\left[\hat{C}_{42}, \tilde{C}_{21}^2\right]}{E\left[\hat{C}_{42}\right] E\left[\tilde{C}_{21}^2\right]} + \frac{Var\left[\tilde{C}_{21}^2\right]}{E\left[\tilde{C}_{21}^2\right]^2}\right]. \quad (21)$$

The general expression of the variance of the fourth-order cumulant, $\hat{C}_{42}$, is obtained as (A.32)

$$Var\left[\hat{C}_{42}\right] \approx \frac{M_{84}}{K} - \frac{8M_{63}M_{21}}{K} - \frac{M_{42}^2}{K} + \frac{24M_{21}^2 M_{42}}{K} + \frac{2M_{42}|M_{20}|^2}{K} + \frac{2\mathrm{Re}\left[M_{40}\left(M_{20}^2\right)^*\right]}{K} - \frac{16M_{21}^4}{K} - \frac{4|M_{20}|^4}{K}. \quad (22)$$

Substituting the values obtained from (17)–(19) and (22) into (21), we calculate the final expression of the variance of the estimated normalized fourth-order cumulant of $\tilde{C}_{42}$.

At the first stage, by employing $\tilde{C}_{42_R}$ we have the distinct features for the MSK, 16-QAM, and OQPSK modulations. Fig. 3 (a) shows the histogram of $\tilde{C}_{42_R}$ for the different modulation formats at 20 dB SNR, where (μ_1, σ_1^2), (μ_2, σ_2^2), (μ_3, σ_3^3), (μ_4, σ_4^2), and (μ_5, σ_5^2) are the mean and variance value for MSK, QPSK, BPSK, 16-QAM, and OQPSK modulations, respectively, discussed in Appendix B. The decision rule used to classify these modulations is

$$\begin{aligned} \tilde{C}_{42_R} &< \eta_1 \Rightarrow \mathrm{MSK} \\ \eta_1 \le \tilde{C}_{42_R} &< \eta_2 \Rightarrow \mathrm{BPSK\ and\ QPSK} \\ \eta_2 \le \tilde{C}_{42_R} &< \eta_3 \Rightarrow 16-\mathrm{QAM} \\ \tilde{C}_{42_R} &\ge \eta_3 \Rightarrow \mathrm{OQPSK}, \end{aligned} \quad (23)$$

where η_1, η_2, and η_3 are the thresholds, discussed in Appendix B.

It is observed that at the first stage, we cannot classify BPSK and QPSK modulation formats as they have almost the same fourth-order cumulant values. At the second stage, to get the distinct features for BPSK and QPSK modulations, we have used DFT of square of the received signal with the normalized fourth-order cumulant. Fig. 3(b) shows the histogram of $\tilde{C}_{42_U}$ for BPSK and QPSK modulation formats at 20 dB SNR, where $(\bar{\mu}_2, \bar{\sigma}_2^2)$ and $(\bar{\mu}_3, \bar{\sigma}_3^2)$ are the mean and variance value for QPSK and BPSK modulations, respectively, discussed in the Appendix B. The decision rule used is

$$\begin{aligned} \tilde{C}_{42_U} &< \eta_4 \Rightarrow \mathrm{QPSK} \\ \tilde{C}_{42_U} &\ge \eta_4 \Rightarrow \mathrm{BPSK}, \end{aligned} \quad (24)$$

where η_4 is the threshold, discussed in the Appendix B.

Remark: By substituting $\theta_u = 0$ in (11) and (15), we can observe that, in the exponential term only timing offset (τ) is left as dependent term. For an OFDM block τ is fixed, if τ is small, the cumulant values lies between η_1 and η_2 and when τ is large then the cumulant values fall outside the threshold region, i.e., greater than η_2 as shown in Fig. 3 (c) for the QPSK modulated signal. Similarly, for the other modulation formats, the threshold cannot be estimated properly as it varies with τ. However, in the proposed algorithm to nullify the effect of timing offset, we have introduced uniformly distributed random timing offsets, θ_u, in each of the OFDM symbols as shown in Fig. 2. In this case $\tau + \theta_u$ will be a new uniform random variable whose mean and variance at the first stage and second stage is given by $\{(\mu_1, \sigma_1^2), (\mu_2, \sigma_2^2), (\mu_3, \sigma_3^3), (\mu_4, \sigma_4^2), (\mu_5, \sigma_5^2)\}$ and $\{(\bar{\mu}_2, \bar{\sigma}_2^2), (\bar{\mu}_3, \bar{\sigma}_3^2)\}$, respectively. After taking the statistical average over OFDM symbols, cumulant values $\tilde{C}_{42_R}$ and $\tilde{C}_{42_U}$, lies within the thresholds, i.e., we will get the unique features for different modulation formats as shown in Fig. 3(a) and (b).

Authorized licensed use limited to: Indian Institute of Technology Patna. Downloaded on January 16,2024 at 05:46:31 UTC from IEEE Xplore. Restrictions apply.

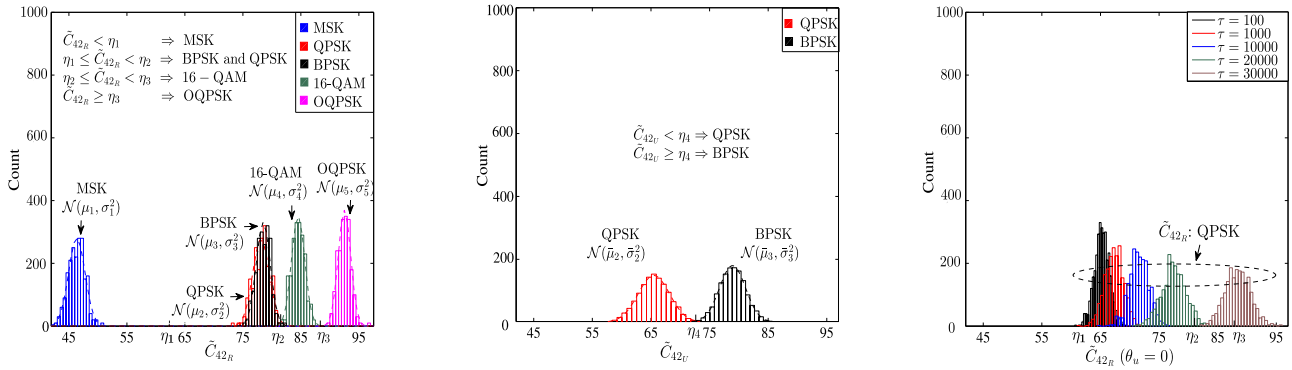

Fig. 3. Histogram of the normalized fourth-order cumulant at SNR $= 20$ dB and $L = 4$ with Rayleigh fading: (a) First stage classification, (b) Second stage classification, and (c) Histogram of QPSK modulated signal without introducing uniformly distributed timing offsets, i.e., $\theta_u = 0$.

TABLE I
COMPLEXITY ANALYSIS

Methods	Order of Complexity
Higher-order cumulant	$\mathcal{O}(M)$ [13], [29]
Kolmogorov-Smirnov (KS) test	$\mathcal{O}(M\log M)$ [29]
Proposed algorithm	$\mathcal{O}(M^2\log M)$
Maximum likelihood (ML)	$\mathcal{O}(M \times A_c \times J)$ [27]

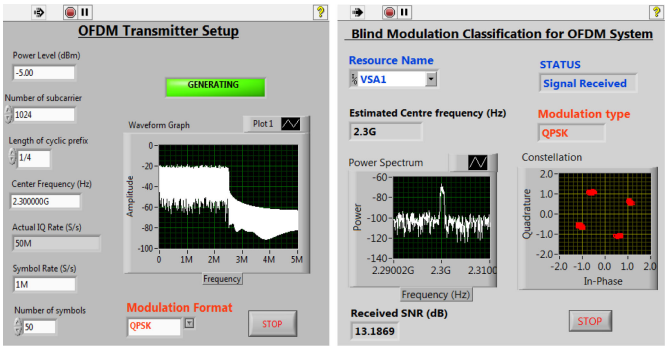

Fig. 4. LabVIEW front panel of OFDM system: (a) the transmitter setup using NI PXIe-5673 and (b) the receiver setup using NI PXIe-5663.

C. Complexity Analysis

The computational complexity of the proposed and existing algorithms are provided in Table I.

The constellation size of the cth modulation format is A_c and J is the total number of modulations considered for classification. The complexity order of the proposed MC algorithm is greater than the algorithms based on the KS-test and higher-order cumulant, but less than that of the ML algorithm. However, the algorithms based on the ML, KS-test and higher-order cumulant require known channel and/or perfect synchronization conditions. Moreover, these methods cannot classify the variants of QPSK, i.e., OQPSK and MSK modulation formats.

Algorithm 1: Proposed Modulation Classification Algorithm.

Input: The received OFDM symbols $r_m[k]$ in the presence of synchronization errors, i.e., timing, frequency, and phase offsets without the prior knowledge of the channel statistics.

- First, we introduce uniformly distributed timing offsets, θ_u, in each of the OFDM symbols.

Stage 1:

- Compute the DFT, $\bar{R}_m[v]$, of the modified OFDM signal, $\bar{r}_m[k]$.
- Take the statistical average of all the normalized fourth-order cumulant, i.e., $\tilde{C}_{42_R}$ given in (11).
- OQPSK, MSK, and 16-QAM modulations are classified using different thresholds.

Stage 2:

- Compute the DFT, $\bar{U}_m[v]$, of the square of the modified signal, i.e., $\bar{r}_m^2[k]$.
- Similarly, take the statistical average of all the normalized fourth-order cumulant, i.e., $\tilde{C}_{42_U}$ given in (15).
- Now, we have distinct features for BPSK and QPSK modulation formats.

IV. IMPLEMENTATION AND MEASUREMENT SETUP

The implementation and measurement have been performed in signal processing for wireless communication laboratory, IIT Patna. Both transmitter and receiver are configured by software programmable NI PXIe-5673 vector signal generator (VSG) and NI PXIe-5663 vector signal analyzer (VSA) respectively with NI PXIe-1085 chassis [2], [35]. At the transmitter, modulated OFDM signals are generated by NI PXIe-5673 VSG, which consists of NI PXIe-5450 waveform generator, NI PXIe-5652 local oscillator, and NI PXIe-5611 radio frequency (RF) upconverter connected with VERT-2450 antenna to transmit the signal through the air. Fig. 4(a) shows the front panel of the transmitter setup using PXIe-5673 and Fig. 4(b) presents the LabVIEW

Authorized licensed use limited to: Indian Institute of Technology Patna. Downloaded on January 16,2024 at 05:46:31 UTC from IEEE Xplore. Restrictions apply.

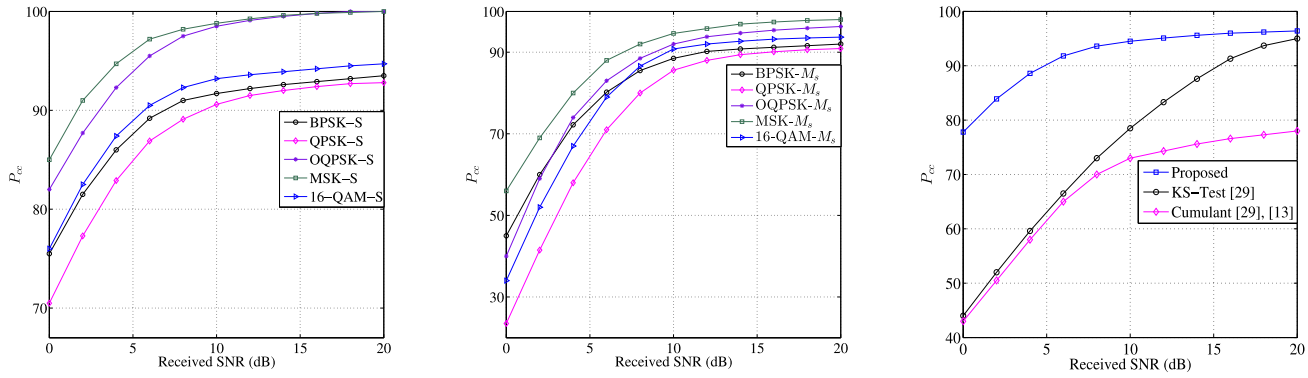

Fig. 5. P_{cc} vs. SNR for {BPSK, QPSK, OQPSK, MSK, 16-QAM} modulation formats: (a) Simulation (S) results and (b) Measurement (M_s) results. (c) Simulation results comparison: P_{cc} vs. SNR for {BPSK, QPSK, 16-QAM} modulation formats.

front panel of the receiver testbed using NI PXIe-5663. It consists of NI PXIe-5622 intermediate frequency (IF) digitizer, NI PXIe-5652 local oscillator, and PXIe-5601 RF downconverter. The signal analyzer process is divided into two parts: RF signal acquisition and IF-baseband signal processing. It presents an instantaneous performance of the proposed MC algorithm for the OFDM system, where the modulation type, received SNR, and RF carrier frequency are estimated. The software used to configure the transmitter and receiver are LabVIEW and MATLAB.

RF Signal Acquisition: This process is controlled by the LabVIEW signal analyzer modules. First, the received OFDM signals are passed through a specified filter span to receive the signals within a particular band. By keeping the transmitter idle, a predefined threshold is captured through a calibration process. After that, the energy of the received OFDM signal is determined and compared with a predefined threshold. If the energy is above the threshold value, the location of the peak is detected, i.e., the estimated RF carrier frequency; alternatively, repeat the same process for the next signal burst. After the estimation of RF carrier frequency, the received RF signal is downconverted to IF signal.

IF-Baseband Signal Processing: The IF-baseband signal processing is controlled by LabVIEW MathScript real-time module. The received IF signal is fed to the MATLAB script, which runs inside the LabVIEW environment. First, the IF carrier frequency and signal bandwidth are estimated from the power spectral density of the signal discussed in [5] then by another downconversion process, we get the baseband signal. Now, the MC algorithm is performed in two stages as described in Section III to classify five-class of modulation formats.

V. Simulation and Measurement Results

In this section, the simulations and measurement performance of the proposed MC algorithm are evaluated using Monte Carlo simulations. In the simulations, Rayleigh frequency-selective fading channel with exponential power delay profile (PDP) and $L=4$ channel taps is implemented. The impairments, i.e., timing, phase, and frequency offset are introduced in the simulation as $\tau \in [-K/2, K/2]$, $\phi \in [-\pi, \pi)$, and $f_o \in [-0.5, 0.5]$, respectively. During measurement, the RF carrier frequency is set to 2.3 GHz. The number of subcarriers, IF carrier frequency, receiver sampling rate and symbol rate are 1024, 5 MHz, 50 MHz, and 1 MHz, respectively. The number of OFDM symbols for each iteration is set to 50 and the performance is measured from 10000 iterations.

Figs. 5(a) and (b) present the percentage of correct classification (P_{cc}) versus received SNR of the proposed MC algorithm for five modulation schemes, i.e., BPSK, QPSK, OQPSK, MSK, and 16-QAM. It has been observed that up to 10 dB SNR, performance increases exponentially and after that, it is almost steady. It has been noticed that the classification accuracy through simulation is better than the measurement. This deviation in the measurement performance is due to the RF hardware impairment [35]. Also, the channel condition in both simulation and measurement environment is not exact, which also affects the classification performance in the simulation and measurement results.

Fig. 5(c) presents the simulation result of the proposed algorithm and compares with existing algorithms. It is noticed that the proposed MC algorithm outperforms the KS test [29] and cumulant-based [13], [29] algorithms. However, these algorithms require perfect timing synchronization as compared to the proposed one which works for unknown timing, frequency, and phase offset. Moreover, these methods are able to classify BPSK, QPSK, and 16-QAM modulations only, whereas the proposed MC algorithm is also applicable to OQPSK and MSK modulations. Additionally, the other existing algorithms for OFDM systems [27], [28], [30], [31], cannot work in the presence of synchronization errors and also requires knowledge of CSI.

Fig. 6(a) presents the P_{cc} versus SNR, for distinct values of M, i.e., 10, 30, 50, and 70. It has been observed that a substantial improvement in the performance is attained as M increases. For higher classification accuracy, the value of M is kept greater than 30.

Fig. 6(b) shows the P_{cc} versus SNR, for asynchronous OFDM under different fading conditions, i.e., Nakagami-m, $m = 1$

Authorized licensed use limited to: Indian Institute of Technology Patna. Downloaded on January 16,2024 at 05:46:31 UTC from IEEE Xplore. Restrictions apply.

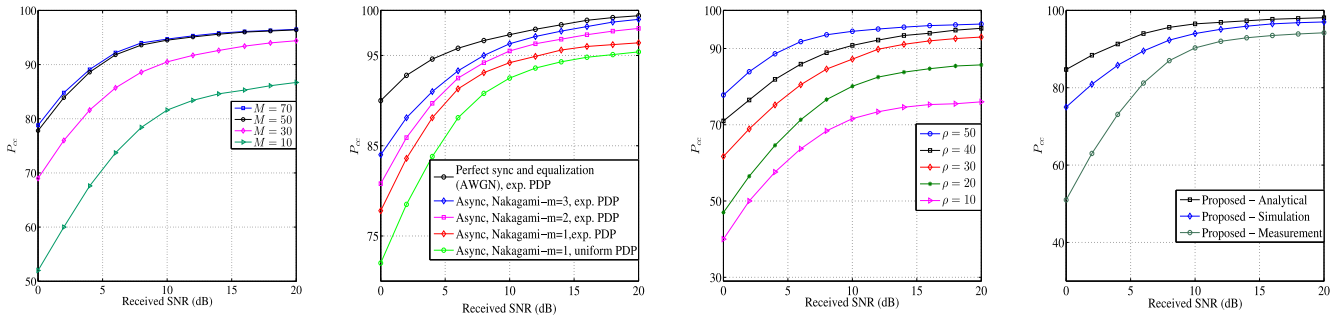

Fig. 6. (a) Simulation results: Effect of M on P_{cc} for five-class of modulation formats. (b) Simulation results comparison: P_{cc} vs. SNR under different fading environment with synchronous and asynchronous OFDM system for five-class of modulation formats. (c) Simulation results: Effect of ρ on P_{cc} for five-class of modulation formats. (d) Analytical, Simulation, and Measurement results: P_{cc} vs. SNR for five-class of modulation formats.

(Rayleigh), $m = 2$, and $m = 3$ for exponential and uniformly distributed PDP. In addition, we also compared the performance of the proposed algorithm with the perfectly synchronized and equalized OFDM signal. Moreover, by comparing the results in Fig. 6(b), it is noted that improved results are attained for $m = 3, 2$ compared to $m = 1$, as expected. Furthermore, the exponential PDP has a slightly better classification performance than the uniform PDP because, for the exponential PDP, the power of the first path, i.e., line of sight component, is usually much greater than that of the other paths, which is not the case in uniform PDP.

Fig. 6(c) shows the P_{cc} versus SNR, for different values of ρ, i.e., 10, 20, 30, 40, and 50. It is observed that the optimum value of the oversampling factor that we can choose is between 30 to 50 for better classification performance.

Fig. 6(d) shows the overall success rate of the proposed algorithm through analytical, simulations, and measurements. It has been observed that the difference in analytical and simulation performance. Because in the analysis the variance of the different modulation formats is considered almost alike, which is usually not the case in the simulations. Moreover, the performance deviation in the experiment is mainly due to RF hardware impairment in the NI vector signal generator and analyzer, i.e., quadrature skew, gain imbalance, and DC offset.

VI. Conclusion

In this paper, we introduced a feature-based blind MC algorithm for an OFDM system in the presence of synchronization errors, i.e., frequency, timing, and phase offsets and without the prior information about the channel statistics and other signal parameters. The proposed algorithm utilizes the combined properties of DFT and the normalized fourth-order cumulant of the received OFDM signal. The results show that the proposed algorithm can achieve better classification performance as compared to the existing algorithms for OFDM systems, and is also able to classify a more comprehensive pool of modulations, i.e., BPSK, QPSK, OQPSK, MSK, and 16-QAM. The work is validated by providing experimental results using NI testbed setup over an indoor propagation environment. As part of future work, we plan to propose a blind MC algorithm for a MIMO-OFDM system.

Appendix A

In this section, we derive the general expression of the mean, variance, and co-variance of the estimates of the second and fourth-order cumulants. For complex-valued random processes $X_m[v] = \{\bar{R}_m[v] \text{or} \bar{U}_m[v]\}$, mixed moments of order x with y conjugations for $X_m[v]$ is defined as $M_{xy_{X_m}} = E[X_m[v]^{x-y} X_m^*[v]^y]$. For the ease of representation we can write the generalized cumulant of $\tilde{C}_{xy_{X_m}}$ as $\tilde{C}_{xy}$ and moment of $M_{xy_{X_m}}$ as M_{xy}. From [13], invoking the central limit theorem, $\hat{M}_{xy}$ is an unbiased estimator and asymptotically Gaussian at high SNR, with mean $E[\hat{M}_{xy}] = M_{xy}$ and variance $Var[\hat{M}_{xy}] = (M_{2x,x} - |M_{xy}|^2)/K$. The mean and variance of the second and fourth-order estimates is given as $E[\hat{C}_{21}] = E[\hat{M}_{21}] = M_{21}$, $E[\hat{C}_{20}] = E[\hat{M}_{20}] = M_{20}$, $E[\hat{M}_{42}] = M_{42}$, $Var[\hat{M}_{21}] = (M_{42} - M_{21}^2)/K$, and $Var[\hat{M}_{42}] = (M_{84} - M_{42}^2)/K$. By using Taylor series approximation, the general expression of the second-order estimator of the mean value of the normalized fourth-order cumulant, $\tilde{C}_{42}$, is expressed as in (16)

$$E\left[\tilde{C}_{42}\right] = \frac{E\left[\hat{C}_{42}\right]}{E\left[\tilde{C}_{21}^2\right]}\left[1 - \frac{Cov\left[\hat{C}_{42}, \tilde{C}_{21}^2\right]}{E\left[\hat{C}_{42}\right] E\left[\tilde{C}_{21}^2\right]} + \frac{Var\left[\tilde{C}_{21}^2\right]}{E\left[\tilde{C}_{21}^2\right]^2}\right]. \tag{A.1}$$

First, we calculate the expected value of $\hat{C}_{42}$ as

$$E\left[\hat{C}_{42}\right] = E\left[\hat{M}_{42}\right] - 2E\left[\hat{M}_{21}^2\right] - E\left[|\hat{M}_{20}|^2\right]. \tag{A.2}$$

Now, we find the expected value of $\hat{M}_{21}^2$ and $|\hat{M}_{20}|^2$ as

$$\begin{aligned} E\left[\hat{M}_{21}^2\right] &= E\left[\left(\frac{1}{K}\sum_{a=1}^{K}|X_m[a]|^2\right)\left(\frac{1}{K}\sum_{b=1}^{K}|X_m[b]|^2\right)\right], \\ &= \frac{1}{K^2}E\left[\sum_{a=1}^{K}|X_m[a]|^4 + \sum_{a=1}^{K}\sum_{b=1}^{K}|X_m[a]|^2|X_m[b]|^2\right], \\ &= \frac{M_{42}}{K} + M_{21}^2\frac{K-1}{K}. \end{aligned} \tag{A.3}$$

Authorized licensed use limited to: Indian Institute of Technology Patna. Downloaded on January 16,2024 at 05:46:31 UTC from IEEE Xplore. Restrictions apply.

$$E\left[|\hat{M}_{20}|^2\right] = \frac{1}{K^2}E\left[\sum_{a=1}^{K}|X_m[a]|^4 + \sum_{a=1}^{K}\sum_{b=1}^{K}X_m[a]^2 X_m^*[b]^2\right],$$
$$= \frac{M_{42}}{K} + |M_{20}|^2\frac{K-1}{K}. \quad \text{(A.4)}$$

The expected value of $\hat{C}_{42}$ is obtained by substituting the values of (A.3), (A.4) in (A.2) as

$$E\left[\hat{C}_{42}\right] = M_{42}\left(\frac{K-3}{K}\right) - |M_{20}|^2\left(\frac{K-1}{K}\right) - 2M_{21}^2\left(\frac{K-1}{K}\right). \quad \text{(A.5)}$$

Now, the expected value of $\tilde{C}_{21}^2$ is calculated as

$$E\left[\tilde{C}_{21}^2\right] = E\left[\hat{C}_{21}^2\right] + \sigma_W^4 - 2\sigma_W^2 E\left[\hat{C}_{21}\right],$$
$$= \frac{M_{42}}{K} + M_{21}^2\frac{K-1}{K} + \sigma_W^4 - 2\sigma_W^2 M_{21}. \quad \text{(A.6)}$$

In an asymptotic analysis only $\mathcal{O}(1)$ and $\mathcal{O}(1/K)$ is considered; remaining terms, $\mathcal{O}(1/K^2)$ and $\mathcal{O}(1/K^3)$ can be omitted. Hence, the expected values, $E[\hat{M}_{21}^2]^2$ and $E[|\hat{M}_{20}|^2]^2$ are obtained as

$$E\left[\hat{M}_{21}^2\right]^2 \approx M_{21}^4\frac{K-2}{K} + \frac{2M_{42}M_{21}^2}{K}, \quad \text{(A.7)}$$

$$E\left[|\hat{M}_{20}|^2\right]^2 \approx |M_{20}|^4\frac{K-2}{K} + \frac{2M_{42}|M_{20}|^2}{K}. \quad \text{(A.8)}$$

The general expression of the variance of $\tilde{C}_{21}^2$ is given as

$$Var\left[\tilde{C}_{21}^2\right] = Var\left[\hat{C}_{21}^2\right] + Var\left[\sigma_W^4 - 2\sigma_W^2\hat{C}_{21}\right] + 2Cov\left[\hat{C}_{21}^2, \sigma_W^4 - 2\sigma_W^2\hat{C}_{21}\right],$$
$$= Var\left[\hat{C}_{21}^2\right] + 4\sigma_W^4 Var\left[\hat{C}_{21}\right] - 2\sigma_W^2 E\left[\hat{C}_{21}^3\right] + 2\sigma_W^2 E\left[\hat{C}_{21}^2\right]E\left[\hat{C}_{21}\right]. \quad \text{(A.9)}$$

Now, we find the variance of $\hat{C}_{21}^2$ as

$$Var\left[\hat{C}_{21}^2\right] = Var\left[\hat{M}_{21}^2\right] = E\left[\hat{M}_{21}^4\right] - E\left[\hat{M}_{21}^2\right]^2. \quad \text{(A.10)}$$

The expected value of $\hat{M}_{21}^4$ is calculated as

$$E\left[\hat{M}_{21}^4\right] \approx \frac{1}{K^4}E\left[6\sum_{a=1}^{K}\sum_{b=1}^{K}\sum_{c=1}^{K}|X_m[a]|^2|X_m[b]|^2|X_m[c]|^4 + \sum_{a=1}^{K}\sum_{b=1}^{K}\sum_{c=1}^{K}\sum_{d=1}^{K}|X_m[a]|^2|X_m[b]|^2|X_m[c]|^2|X_m[d]|^2\right],$$
$$\approx 6M_{21}^2M_{42}\frac{K(K-1)(K-2)}{K^4} + M_{21}^4\frac{K(K-1)(K-2)(K-3)}{K^4},$$
$$\approx \frac{6M_{21}^2M_{42}}{K} + M_{21}^4\frac{K-6}{K}. \quad \text{(A.11)}$$

Similarly, we obtain the expected value of $|\hat{M}_{20}|^4$ as

$$E\left[|\hat{M}_{20}|^4\right] \approx \left(4M_{42}|M_{20}|^2 + 2\mathrm{Re}\left[M_{40}\left(M_{20}^2\right)^*\right]\right)\times\frac{K(K-1)(K-2)}{K^4} + |M_{20}|^4\frac{K(K-1)(K-2)(K-3)}{K^4},$$
$$\approx \frac{4M_{42}|M_{20}|^2}{K} + \frac{2\mathrm{Re}\left[M_{40}\left(M_{20}^2\right)^*\right]}{K} + |M_{20}|^4\frac{K-6}{K}. \quad \text{(A.12)}$$

By putting the values of (A.7) and (A.11) in (A.10), to calculate the variance of $\hat{M}_{21}^2$ as

$$Var\left[\hat{M}_{21}^2\right] \approx \frac{4M_{21}^2M_{42}}{K} - \frac{4M_{21}^4}{K}. \quad \text{(A.13)}$$

Similarly, to calculate the variance of $|\hat{M}_{20}|^2$, we take the values from (A.8), (A.12) as

$$Var\left[|\hat{M}_{20}|^2\right] = E\left[|\hat{M}_{20}|^4\right] - E\left[|\hat{M}_{20}|^2\right]^2,$$
$$\approx \frac{2\mathrm{Re}\left[M_{40}\left(M_{20}^2\right)^*\right]}{K} + \frac{2M_{42}|M_{20}|^2}{K} - \frac{4|M_{20}|^4}{K}. \quad \text{(A.14)}$$

Now, the expected value of $\hat{M}_{21}^3$ is obtained as

$$E\left[\hat{M}_{21}^3\right] \approx \frac{1}{K^3}E\left[3\sum_{a=1}^{K}\sum_{b=1}^{K}|X_m[a]|^4|X_m[b]|^2 + \sum_{a=1}^{K}\sum_{b=1}^{K}\sum_{c=1}^{K}|X_m[a]|^2|X_m[b]|^2|X_m[c]|^2\right],$$
$$\approx 3M_{42}M_{21}\frac{K(K-1)}{K^3} + M_{21}^3\frac{K(K-1)(K-2)}{K^3},$$
$$\approx 3\frac{M_{42}M_{21}}{K} + M_{21}^3\frac{K-3}{K}. \quad \text{(A.15)}$$

Substituting (A.3), (A.15) and (A.13), in (A.9) to obtain the final expression of the variance of $\tilde{C}_{21}^2$ as

$$Var\left[\tilde{C}_{21}^2\right] \approx \left(M_{21} - \sigma_W^2\right)^2\frac{M_{42} - M_{21}^2}{K}. \quad \text{(A.16)}$$

The general expression of the co-variance of $[\hat{C}_{42}, \tilde{C}_{21}^2]$ is given as

$$Cov\left[\hat{C}_{42}, \tilde{C}_{21}^2\right] = E\left[\hat{C}_{42}\tilde{C}_{21}^2\right] - E\left[\hat{C}_{42}\right]E\left[\tilde{C}_{21}^2\right],$$
$$= E\left[\hat{C}_{42}\hat{C}_{21}^2\right] - E\left[\hat{C}_{42}\right]E\left[\hat{C}_{21}^2\right] - 2\sigma_W^2\left[E[\hat{C}_{42}\hat{C}_{21}] - E[\hat{C}_{42}]E[\hat{C}_{21}]\right]. \quad \text{(A.17)}$$

Authorized licensed use limited to: Indian Institute of Technology Patna. Downloaded on January 16,2024 at 05:46:31 UTC from IEEE Xplore. Restrictions apply.

To calculate the expected value of $\hat{C}_{42}\hat{C}_{21}^2$, we have

$$E\left[\hat{C}_{42}\hat{C}_{21}^2\right] = E\left[\hat{M}_{42}\hat{M}_{21}^2\right] - 2E\left[\hat{M}_{21}^4\right] - E\left[\hat{M}_{21}^2|\hat{M}_{20}|^2\right]. \tag{A.18}$$

Now, the expected value of $\hat{M}_{42}\hat{M}_{21}^2$ is obtained as

$$\begin{aligned} E\left[\hat{M}_{42}\hat{M}_{21}^2\right] &\approx \left(M_{42}^2 + 2M_{63}M_{21}\right)\frac{K(K-1)}{K^3} \\ &\quad + M_{42}M_{21}^2\frac{K(K-1)(K-2)}{K^3}, \\ &\approx \frac{M_{42}^2}{K} + \frac{2M_{63}M_{21}}{K} + M_{42}M_{21}^2\frac{K-3}{K}. \end{aligned} \tag{A.19}$$

Similarly, we find the expected value of $\hat{M}_{21}^2|\hat{M}_{20}|^2$ as

$$\begin{aligned} E\left[\hat{M}_{21}^2|\hat{M}_{20}|^2\right] &\approx \frac{M_{42}|M_{20}|^2}{K} + \frac{M_{42}M_{21}^2}{K} \\ &\quad + M_{21}^2|M_{20}|^2\frac{K-2}{K}. \end{aligned} \tag{A.20}$$

After substituting (A.11), (A.19) and (A.20) in (A.18), we get the the expected value of $\hat{C}_{42}\hat{C}_{21}^2$ as

$$\begin{aligned} E\left[\hat{C}_{42}\hat{C}_{21}^2\right] &\approx \frac{M_{42}^2}{K} + \frac{2M_{63}M_{21}}{K} + M_{42}M_{21}^2\frac{K-16}{K} \\ &\quad - 2M_{21}^4\frac{K-6}{K} - \frac{M_{42}|M_{20}|^2}{K} \\ &\quad - M_{21}^2|M_{20}|^2\frac{K-2}{K}. \end{aligned} \tag{A.21}$$

Now, we calculate the expected value of $\hat{C}_{42}\hat{C}_{21}$, as

$$E\left[\hat{C}_{42}\hat{C}_{21}\right] = E\left[\hat{M}_{42}\hat{M}_{21}\right] - 2E\left[\hat{M}_{21}^3\right] - E\left[|\hat{M}_{20}|^2\hat{M}_{21}\right]. \tag{A.22}$$

Similarly, we find the expected value of $|\hat{M}_{20}|^2\hat{M}_{21}$ and $\hat{M}_{42}\hat{M}_{21}$ as

$$E\left[|\hat{M}_{20}|^2\hat{M}_{21}\right] = \frac{M_{42}M_{21}}{K} + |\hat{M}_{20}|^2\hat{M}_{21}\frac{K-1}{K}, \tag{A.23}$$

$$E\left[\hat{M}_{42}\hat{M}_{21}\right] = \frac{M_{63}}{K} + M_{42}M_{21}\frac{K-1}{K}. \tag{A.24}$$

After putting (A.15), (A.23) and (A.24) in (A.22) to get the expected value of $\hat{C}_{42}\hat{C}_{21}$ as

$$\begin{aligned} E\left[\hat{C}_{42}\hat{C}_{21}\right] &\approx \frac{M_{63}}{K} + M_{42}M_{21}\frac{K-8}{K} - 2M_{21}^3\frac{K-3}{K} \\ &\quad - |\hat{M}_{20}|^2\hat{M}_{21}\frac{K-1}{K}. \end{aligned} \tag{A.25}$$

Substituting (A.3), (A.5), (A.21) and (A.25) in (A.17), the expression for the co-variance of $\hat{C}_{42}, \tilde{C}_{21}^2$ is calculated as

$$\begin{aligned} Cov\left[\hat{C}_{42}, \tilde{C}_{21}^2\right] &\approx \frac{2M_{63}M_{21}}{K} - \frac{10M_{42}M_{21}^2}{K} - \frac{2M_{63}\sigma_W^2}{K} \\ &\quad + \frac{8M_{21}^4}{K} + \frac{10M_{42}M_{21}\sigma_W^2}{K} - \frac{8M_{21}^3\sigma_W^2}{K}. \end{aligned} \tag{A.26}$$

Finally, after substituting the values obtained from (A.5), (A.6), (A.16) and (A.26) into (A.1) we calculate the final expression of the mean of the estimated normalized fourth-order cumulant $\tilde{C}_{42}$.

By using Taylor series approximation, the general expression of the first-order estimator of the variance of $\tilde{C}_{42}$ is given as in (21)

$$\begin{aligned} Var\left[\tilde{C}_{42}\right] &= \frac{E\left[\hat{C}_{42}\right]^2}{E\left[\tilde{C}_{21}^2\right]^2}\left[\frac{Var\left[\hat{C}_{42}\right]}{E\left[\hat{C}_{42}\right]^2} - 2\frac{Cov\left[\hat{C}_{42}, \tilde{C}_{21}^2\right]}{E\left[\hat{C}_{42}\right]E\left[\tilde{C}_{21}^2\right]}\right. \\ &\quad \left. + \frac{Var\left[\tilde{C}_{21}^2\right]}{E\left[\tilde{C}_{21}^2\right]^2}\right]. \end{aligned} \tag{A.27}$$

The variance of $\hat{C}_{42}$ is expressed as

$$\begin{aligned} Var\left[\hat{C}_{42}\right] &= Var\left[\hat{M}_{42} - 2\hat{M}_{21}^2\right] + Var\left[|\hat{M}_{20}|^2\right] \\ &\quad - 2Cov\left[\left(\hat{M}_{42} - 2\hat{M}_{21}^2\right), \left(|\hat{M}_{20}|^2\right)\right]. \end{aligned} \tag{A.28}$$

Now, we calculate the variance of $\hat{M}_{42} - 2\hat{M}_{21}^2$ as

$$\begin{aligned} Var\left[\hat{M}_{42} - 2\hat{M}_{21}^2\right] &= Var\left[\hat{M}_{42}\right] + 4Var\left[\hat{M}_{21}^2\right] \\ &\quad - 4Cov\left[\hat{M}_{42}, \hat{M}_{21}^2\right]. \end{aligned} \tag{A.29}$$

Taking equation (A.3) and (A.19), the co-variance of $[\hat{M}_{42}, \hat{M}_{21}^2]$ is obtained as

$$\begin{aligned} Cov\left[\hat{M}_{42}, \hat{M}_{21}^2\right] &= E\left[\hat{M}_{42}\hat{M}_{21}^2\right] - E\left[\hat{M}_{42}\right]E\left[\hat{M}_{21}^2\right], \\ &\approx \frac{2M_{63}M_{21}}{K} - \frac{2M_{42}M_{21}^2}{K}. \end{aligned} \tag{A.30}$$

Similarly, we calculate the estimate of the co-variance of $[(\hat{M}_{42} - 2\hat{M}_{21}^2), |\hat{M}_{20}|^2]$, and it equals to zero. Now, substituting (A.13) and (A.30) in (A.29) we get

$$\begin{aligned} Var\left[\hat{M}_{42} - 2\hat{M}_{21}^2\right] &\approx \frac{M_{84}}{K} - \frac{M_{42}^2}{K} - \frac{16M_{21}^4}{K} \\ &\quad + \frac{24M_{21}^2M_{42}}{K} - \frac{8M_{63}M_{21}}{K}. \end{aligned} \tag{A.31}$$

Substituting (A.14) and (A.31) in A.28, the variance of $\hat{C}_{42}$ is obtained as

$$\begin{aligned} Var\left[\hat{C}_{42}\right] &\approx \frac{M_{84}}{K} - \frac{8M_{63}M_{21}}{K} - \frac{M_{42}^2}{K} + \frac{24M_{21}^2M_{42}}{K} \\ &\quad + \frac{2M_{42}|M_{20}|^2}{K} + \frac{2\mathrm{Re}\left[M_{40}\left(M_{20}^2\right)^*\right]}{K} \\ &\quad - \frac{16M_{21}^4}{K} - \frac{4|M_{20}|^4}{K}. \end{aligned} \tag{A.32}$$

Finally, after substituting the values obtained from (A.5), (A.6), (A.16), (A.26) and (A.32) into (A.27) we calculate the final expression of the variance of the estimated normalized fourth-order cumulant $\tilde{C}_{42}$.

Authorized licensed use limited to: Indian Institute of Technology Patna. Downloaded on January 16,2024 at 05:46:31 UTC from IEEE Xplore. Restrictions apply.

APPENDIX B

In general, we represent mean and variance at the first stage classification as $\mu_{\mathcal{M}} = E[\tilde{C}_{42_R}]$ and $\sigma^2_{\mathcal{M}} = Var[\tilde{C}_{42_R}]$, respectively, where $\mathcal{M} = \{1, 2, 3, 4, 5\}$ belongs to MSK, QPSK, BPSK, 16-QAM, and OQPSK modulation formats, respectively. Similarly, at the second stage, mean is represented by $\bar{\mu}_{\bar{\mathcal{M}}}$ and variance $\bar{\sigma}^2_{\bar{\mathcal{M}}}$, where $\bar{\mathcal{M}} = \{2, 3\}$ belongs to QPSK and BPSK modulation formats, respectively.

The threshold values, i.e., η_1, η_2, η_3, and η_4 are calculated by using the likelihood ratio test. We have the probability density function for MSK, QPSK, BPSK, 16-QAM, and OQPSK modulation formats at the first stage as

$$p(\tilde{C}_{42_R}|\mathcal{M}) = \frac{1}{\sqrt{2\pi\sigma^2_{\mathcal{M}}}} \exp\left[\frac{-(\tilde{C}_{42_R} - \mu_{\mathcal{M}})^2}{2\sigma^2_{\mathcal{M}}}\right]. \quad \text{(B.1)}$$

In an asymptotic threshold value analysis, the variance of the different modulation formats are considered almost alike, equals σ^2 at high SNR. At the first stage classification, as shown in Fig. 3 the mean values obtained for QPSK and BPSK are almost the same, i.e., $\mu_2 \approx \mu_3$. The likelihood ratio of MSK and QPSK/BPSK is given by

$$\Lambda(\tilde{C}_{42_R}) = \exp\left[\frac{(\tilde{C}_{42_R} - \mu_1)^2 - (\tilde{C}_{42_R} - \mu_2)^2}{2\sigma^2}\right]$$
$$= \exp\left[\left(\frac{\mu_2 - \mu_1}{\sigma^2}\right)\left(\tilde{C}_{42_R} - \frac{\mu_2 + \mu_1}{2}\right)\right]. \quad \text{(B.2)}$$

To calculate η_1, we have

$$\exp\left[\left(\frac{\mu_2 - \mu_1}{\sigma^2}\right)\left(\tilde{C}_{42_R} - \frac{\mu_2 + \mu_1}{2}\right)\right] \underset{\text{MSK}}{\overset{\text{QPSK, BPSK}}{\gtrless}} \Psi_1, \quad \text{(B.3)}$$

where Ψ_1 is the ratio of the prior probabilities of MSK and QPSK/BPSK modulation formats. This can be further simplified as

$$\tilde{C}_{42_R} \underset{\text{MSK}}{\overset{\text{QPSK, BPSK}}{\gtrless}} \frac{\sigma^2 \ln(\Psi_1)}{\mu_2 - \mu_1} + \frac{\mu_2 + \mu_1}{2} = \eta_1. \quad \text{(B.4)}$$

Similarly, we can calculate the threshold values η_2, η_3, and η_4 as

$$\tilde{C}_{42_R} \underset{\text{QPSK, BPSK}}{\overset{\text{16-QAM}}{\gtrless}} \frac{\sigma^2 \ln(\Psi_2)}{\mu_4 - \mu_2} + \frac{\mu_4 + \mu_2}{2} = \eta_2,$$

$$\tilde{C}_{42_R} \underset{\text{16-QAM}}{\overset{\text{OQPSK}}{\gtrless}} \frac{\sigma^2 \ln(\Psi_3)}{\mu_5 - \mu_4} + \frac{\mu_5 + \mu_4}{2} = \eta_3,$$

$$\tilde{C}_{42_U} \underset{\text{QPSK}}{\overset{\text{BPSK}}{\gtrless}} \frac{\sigma^2 \ln(\Psi_4)}{\bar{\mu}_3 - \bar{\mu}_2} + \frac{\bar{\mu}_3 + \bar{\mu}_2}{2} = \eta_4, \quad \text{(B.5)}$$

where Ψ_2 is the ratio of the prior probabilities of QPSK/BPSK and 16-QAM and Ψ_3 is the ratio of the prior probabilities of 16-QAM and OQPSK modulation formats at the first stage classification. Ψ_4 is the ratio of the prior probabilities of QPSK and BPSK modulations at the second stage classification. The error probability for MSK modulation format is given as,

$$\Pr(e \,|\, \text{MSK}) = \Pr(\tilde{C}_{42_R} \geq \eta_1 \,|\, \text{MSK})$$

$$\Pr\left(\tilde{C}_{42_R} \geq \eta_1 \,|\, \text{MSK}\right) = \Pr\left(\frac{\tilde{C}_{42_R} - \mu_1}{\sigma} \geq \frac{\eta_1 - \mu_1}{\sigma} \,|\, \text{MSK}\right),$$
$$= Q\left(\frac{\eta_1 - \mu_1}{\sigma}\right), \quad \text{(B.6)}$$

where $Q(\cdot)$ is the complementary distribution function. Replacing η_1 by its value in (B.4), we get

$$\Pr(e \,|\, \text{MSK}) = Q\left(\frac{\sigma \ln(\Psi_1)}{\mu_2 - \mu_1} + \frac{\mu_2 - \mu_1}{2\sigma}\right). \quad \text{(B.7)}$$

Similarly, we get the error probabilities for 16-QAM modulation formats as

$$\Pr(e \,|\, \text{16-QAM}) = Q\left(\frac{-\sigma \ln(\Psi_2)}{\mu_4 - \mu_2} + \frac{\mu_4 - \mu_2}{2\sigma}\right), \quad \text{(B.8)}$$

and

$$\Pr(e \,|\, \text{16-QAM}) = Q\left(\frac{\sigma \ln(\Psi_3)}{\mu_5 - \mu_4} + \frac{\mu_5 - \mu_4}{2\sigma}\right). \quad \text{(B.9)}$$

The error probabilties for OQPSK, QPSK, and BPSK are given in (B.10), (B.11), and (B.12), respectively, as

$$\Pr(e \,|\, \text{OQPSK}) = Q\left(\frac{-\sigma \ln(\Psi_3)}{\mu_5 - \mu_4} + \frac{\mu_5 - \mu_4}{2\sigma}\right), \quad \text{(B.10)}$$

$$\Pr(e \,|\, \text{QPSK}) = Q\left(\frac{\sigma \ln(\Psi_4)}{\bar{\mu}_3 - \bar{\mu}_2} + \frac{\bar{\mu}_3 - \bar{\mu}_2}{2\sigma}\right), \quad \text{(B.11)}$$

$$\Pr(e \,|\, \text{BPSK}) = Q\left(\frac{-\sigma \ln(\Psi_4)}{\bar{\mu}_3 - \bar{\mu}_2} + \frac{\bar{\mu}_3 - \bar{\mu}_2}{2\sigma}\right). \quad \text{(B.12)}$$

REFERENCES

[1] O. A. Dobre, A. Abdi, Y. Bar-Ness, and W. Su, "Survey of automatic modulation classification techniques: Classical approaches and new trends," *IET Commun.*, vol. 1, no. 2, pp. 137–156, Apr. 2007.

[2] R. Gupta, S. Majhi, and O. A. Dobre, "Design and implementation of a tree-based blind modulation classification algorithm for multiple-antenna systems," *IEEE Trans. Instrum. Meas.*, vol. 68, no. 8, pp. 3020–3031, Aug. 2019.

[3] S. Majhi, R. Gupta, W. Xiang, and S. Glisic, "Hierarchical hypothesis and feature-based blind modulation classification for linearly modulated signals," *IEEE Trans. Veh. Technol.*, vol. 66, no. 12, pp. 11 057–11 069, Jul. 2017.

[4] J. L. Xu, W. Su, and M. Zhou, "Software-defined radio equipped with rapid modulation recognition," *IEEE Trans. Veh. Technol.*, vol. 59, no. 4, pp. 1659–1667, May 2010.

[5] S. Majhi, M. Kumar, and W. Xiang, "Implementation and measurement of blind wireless receiver for single carrier systems," *IEEE Trans. Instrum. Meas.*, vol. 66, no. 8, pp. 1965–1975, Aug. 2017.

[6] S. Majhi and T. S. Ho, "Blind symbol-rate estimation and testbed implementation of linearly modulated signals," *IEEE Trans. Veh. Technol.*, vol. 64, no. 3, pp. 954–963, Sep. 2015.

[7] T. Hwang, C. Yang, G. Wu, S. Li, and G. Y. Li, "OFDM and its wireless applications: A survey," *IEEE Trans. Veh. Technol.*, vol. 58, no. 4, pp. 1673–1694, May 2009.

[8] Z. Qin, H. Ye, G. Y. Li, and B. F. Juang, "Deep learning in physical layer communications," *IEEE Wireless Commun.*, vol. 26, no. 2, pp. 93–99, Apr. 2019.

[9] G. Gui, H. Huang, Y. Song, and H. Sari, "Deep learning for an effective nonorthogonal multiple access scheme," *IEEE Trans. Veh. Technol.*, vol. 67, no. 9, pp. 8440–8450, Sep. 2018.

[10] S. Chen, Y. Zhang, Z. He, J. Nie, and W. Zhang, "A novel attention cooperative framework for automatic modulation recognition," *IEEE Access*, vol. 8, pp. 15 673–15 686, 2020.

Authorized licensed use limited to: Indian Institute of Technology Patna. Downloaded on January 16,2024 at 05:46:31 UTC from IEEE Xplore. Restrictions apply.

[11] J. Nie, Y. Zhang, Z. He, S. Chen, S. Gong, and W. Zhang, "Deep hierarchical network for automatic modulation classification," *IEEE Access*, vol. 7, pp. 94 604–94 613, Jul. 2019.
[12] W. Wei and J. M. Mendel, "Maximum-likelihood classification for digital amplitude-phase modulations," *IEEE Trans. Commun.*, vol. 48, no. 2, pp. 189–193, Feb. 2000.
[13] A. Swami and B. M. Sadler, "Hierarchical digital modulation classification using cumulants," *IEEE Trans. Commun.*, vol. 48, no. 3, pp. 416–429, Mar. 2000.
[14] H.-C. Wu, M. Saquib, and Z. Yun, "Novel automatic modulation classification using cumulant features for communications via multipath channels," *IEEE Trans. Wireless Commun.*, vol. 7, no. 8, pp. 3098–3105, Aug. 2008.
[15] M. Oner and O. A. Dobre, "On the second-order cyclic statistics of signals in the presence of receiver impairments," *IEEE Trans. Commun.*, vol. 59, no. 12, pp. 3278–3284, Dec. 2011.
[16] S. Majhi, R. Gupta, and W. Xiang, "Novel blind modulation classification of circular and linearly modulated signals using cyclic cumulants," in *Proc. IEEE Annu. Symp. Pers. Indoor Mobile Radio Commun.*, Oct. 2017, pp. 1–5.
[17] R. Gupta, S. Majhi, and O. A. Dobre, "Blind modulation classification of different variants of QPSK and 8-PSK for multiple-antenna systems with transmission impairments," in *Proc. IEEE Veh. Technol. Conf.*, Aug. 2018, pp. 1–5.
[18] P. Daponte, G. Mercurio, and S. Rapuano, "A wavelet networks-based method for the digital telecommunication system monitoring," *IEEE Trans. Instrum. Meas.*, vol. 50, no. 6, pp. 1773–1780, Dec. 2001.
[19] M. W. Aslam, Z. Zhu, and A. K. Nandi, "Automatic modulation classification using combination of genetic programming and KNN," *IEEE Trans. Wireless Commun.*, vol. 11, no. 8, pp. 2742–2750, Aug. 2012.
[20] X. Liu, C. Zhao, P. Wang, Y. Zhang, and T. Yang, "Blind modulation classification algorithm based on machine learning for spatially correlated MIMO system," *IET Commun.*, vol. 11, no. 7, pp. 1000–1007, Dec. 2017.
[21] Y. Wang, M. Liu, J. Yang, and G. Gui, "Data-driven deep learning for automatic modulation recognition in cognitive radios," *IEEE Trans. Veh. Technol.*, vol. 68, no. 4, pp. 4074–4077, Apr. 2019.
[22] F. Meng, P. Chen, L. Wu, and X. Wang, "Automatic modulation classification: A deep learning enabled approach," *IEEE Trans. Veh. Technol.*, vol. 67, no. 11, pp. 10 760–10 772, Nov. 2018.
[23] W. Xie, S. Hu, C. Yu, P. Zhu, X. Peng, and J. Ouyang, "Deep learning in digital modulation recognition using high order cumulants," *IEEE Access*, vol. 7, pp. 63 760–63 766, May 2019.
[24] S. Hong, Y. Zhang, Y. Wang, H. Gu, G. Gui, and H. Sari, "Deep learning-based signal modulation identification in OFDM systems," *IEEE Access*, vol. 7, pp. 114 631–114 638, 2019.
[25] C. Ha, Y. You, and H. Song, "Machine learning model for adaptive modulation of multi-stream in MIMO-OFDM system," *IEEE Access*, vol. 7, pp. 5141–5152, Jan. 2019.
[26] Y. Liu, O. Simeone, A. M. Haimovich, and W. Su, "Modulation classification for MIMO-OFDM signals via approximate Bayesian inference," *IEEE Trans. Veh. Technol.*, vol. 66, no. 1, pp. 268–281, Jan. 2017.
[27] L. Haring, Y. Chen, and A. Czylwik, "Automatic modulation classification methods for wireless OFDM systems in TDD mode," *IEEE Trans. Commun.*, vol. 58, no. 9, pp. 2480–2485, Sep. 2010.
[28] J. Zheng and Y. Lv, "Likelihood-based automatic modulation classification in OFDM with index modulation," *IEEE Trans. Veh. Technol.*, vol. 67, no. 9, pp. 8192–8204, Sep. 2018.
[29] F. Wang and X. Wang, "Fast and robust modulation classification via Kolmogorov-Smirnov test," *IEEE Trans. Commun.*, vol. 58, no. 8, pp. 2324–2332, Aug. 2010.
[30] A. D. Pambudi, S. Tjondronegoro, and H. Wijanto, "Statistical properties proposed for blind classification OFDM modulation scheme," in *Proc. IEEE Int. Conf. Aerosp. Electron. Remote Sens. Technol.*, Nov. 2014, pp. 89–93.
[31] D. Shimbo and I. Oka, "A modulation classification using amplitude moments in OFDM systems," in *Proc. Int. Symp. Inf. Theory Its Appl.*, Oct. 2010, pp. 288–293.
[32] T. Yucek and H. Arslan, "OFDM signal identification and transmission parameter estimation for cognitive radio applications," in *Proc. IEEE Global Telecommun. Conf.*, Nov. 2007, pp. 4056–4060.
[33] D. R. Brillinger, *Time Series: Data Analysis and Theory*. Philadelphia, PA, USA: Soc. Ind. Appl. Math., 2001, vol. 36.
[34] Carnegie Mellon University, Statistics & Data Science. [Online]. Available: http://www.stat.cmu.edu/ hseltman/files/ratio.pdf
[35] National Instruments PXI platform. [Online]. Available: http://www.ni.com

Rahul Gupta received the B.Tech degree in electronics and communication from the Oriental Institute of Science and Technology, Bhopal, India, in 2012 and the M.Tech. and Ph.D. degrees in electrical engineering from the Indian Institute of Technology Patna, Daulatpur, India, in 2015 and 2020, respectively. He is currently a Postdoctoral Researcher with IRIDA Research centre for communication technologies, Department of Electrical and Computer Engineering, University of Cyprus, Nicosia, Cyprus. His research interests include signal processing, wireless communication, estimation and detection theory, higher order statistics, OFDM, MIMO, and MIMO-OFDM and their applications in blind modulation classification and SWIPT.

Sushant Kumar received the B.Tech. degree in electronics and communication from ICFAI University, Dehradun, India, in 2011, and the M.Tech. degree in communication system engineering from the Indian Institute of Technology Patna, Daulatpur, India, in 2015, where he is currently working toward the Ph.D. degree in electrical engineering. His research interests include signal processing, wireless communication, and timing and frequency synchronization in SC-FDMA and MIMO SC-FDMA.

Sudhan Majhi (Senior Member, IEEE) received the M.Tech degree in computer science and data processing from the Indian Institute of Technology, Kharagpur, India, in 2004 and the Ph.D. degree from Nanyang Technological University, Singapore, in 2008. He has Post-doctoral experience with the University of Michigan- Dearborn, MI, USA, Institute of Electronics and Telecommunications, Rennes, France and Nanyang Technological University, Singapore. He is currently an Associate Professor with Department of Electrical Engineering, Indian Institute of Technology, Patna, Daulatpur, India. He is currently a fellow of Sir Visvesvaraya Young Faculty Research. His research interest is signal processing for wireless communication which includes blind synchronization and parameter estimation, cooperative communications, physical layer security for cognitive radio, sequence design, OFDM, MIMO, SC-FDMA, and MIMO-OFDM.

Authorized licensed use limited to: Indian Institute of Technology Patna. Downloaded on January 16,2024 at 05:46:31 UTC from IEEE Xplore. Restrictions apply.